Structure, Bonding, and Reactivity of Tantalum Amides Containing *o*-Naphthyl- and *o*-Indenylphenoxide Ligation

Matthew G. Thorn, Jennifer R. Parker, Phillip E. Fanwick, and Ian P. Rothwell*

Purdue University, Department of Chemistry, 560 Oval Drive, West Lafayette, Indiana 47907-2038

Received February 7, 2003

The reaction of $[Ta(NMe_2)_5]$ with the *o*-(2,3-dihydro-1-naphthyl)-, *o*-(1-naphthyl)-, and *o*-(inden-3-yl)phenols $[HOC_6H_2Ar\text{-}2\text{-}Bu^t_2\text{-}4,6]$ (Ar = $C_{10}H_9$ (**1**), $C_{10}H_7$ (Np; **2**), C_9H_7 (**3**)) has been investigated. In all three cases initial displacement of 1 equiv of dimethylamine occurs, yielding mono(aryloxides) $[(ArO)Ta(NMe_2)_4]$. Structural studies of the *o*-(2,3-dihydro-1-naphthyl) and *o*-(1-naphthyl) compounds **4** and **5** show they both adopt geometries best described as square pyramidal with an apical dimethylamido ligand and basal aryloxide oxygen. The Ta−O−Ar angles are 162° in both compounds, with no metal interaction with the ortho substituents. Compound **4** reacts with 2,3,5,6-tetraphenylphenol to form the corresponding bis(aryloxide) **6**. The intermediate *o*-(inden-3-yl)phenoxide $[(ArO)Ta(NMe_2)_4]$ **7** thermally eliminates a further 1 equiv of $HNMe_2$ with formation of the tris(amido) compound $[Ta(OC_6H_2\{\eta^1\text{-Ind}\}\text{-}2\text{-}Bu^t\text{-}4,6)(NMe_2)_3]$ **8**. The coordination geometry about tantalum in **8** is best described as trigonal bipyramidal, with an oxygen and amido group in the axial positions: O−Ta−N = 170°. The carbon atom of the indenyl ring bound directly to the phenoxide nucleus is metalated, leading to a five-membered metallacycle. Hence, both deprotonation (CH bond activation) and tautomerization of the original inden-3-yl ring has occurred. The Ta−C(121) distance of 2.285(9) Å is consistent with an η^1-indenyl ring being present in **8**. Replacement of the dimethylamido ligands in **8** by chloride groups was achieved by reaction with $SiCl_4$. Structural analysis of the 4-phenylpyridine adduct $[Ta(OC_6H_2\{\eta^3\text{-Ind}\}\text{-}2\text{-}Bu^t\text{-}4,6)(NC_5H_4Ph\text{-}4)Cl_3]$ **9** showed the presence of an η^3-indenyl interaction with the tantalum metal center. The bonding parameters for the η^1- and η^3-indenyl rings are compared with those of related η^5-cyclopentadienyl derivatives of niobium and tantalum.

Introduction

A significant amount of our early research work has focused upon the inorganic and organometallic chemistry of the group 5 metals niobium and tantalum that can be supported by sterically bulky aryloxide ligands.[1] A key feature of *o*-phenylphenoxide ligation has been the involvement of the substituents within the chemistry, including their ability to be reduced (hydrogenated), to chelate via cyclometalation,[2,3] or to form π-bonding interactions with electron-deficient metal centers.[4,5] This has led to our recent interest in the structure and reactivity of aryloxide ligands containing *o*-naphthyl[6] and *o*-indenyl ligation.[7] These substituents introduce a number of interesting stereochemical and structural elements, while the indenyl ligand offers the potential for formation of a constrained-geometry chelate via CH bond activation.[8] In this paper we report on the tantalum amido chemistry of the three related phenols **1**, **2**,[6a] and **3**[7] with emphasis on the structure and fluxionality of the compounds formed as well as the possible bonding modes of the indenylphenoxide ligand.

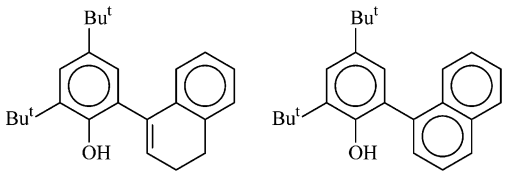

1

2

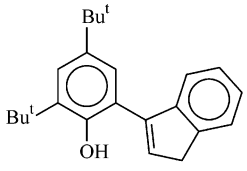

3

* To whom correspondence should be addressed. E-mail: rothwell@purdue.edu.

(1) Bradley, D. C.; Mehrota, R. C.; Rothwell, I. P.; Singh, A. *Alkoxo and Aryloxo Derivatives of Metals*; Academic Press: San Diego, CA, 2001.

(2) (a) Rothwell, I. P. *Acc. Chem. Res.* **1988**, *21*, 153. (b) Lefebvre, F.; Leconte, M.; Pagano, S.; Mutch, A.; Basset, J.-M. *Polyhedron* **1995**, *14*, 3209. (c) Chesnut, R. W.; Durfee, L. D.; Fanwick, P. E.; Rothwell, I. P.; Folting, K.; Huffman, J. C. *Polyhedron* **1987**, *6*, 2019.

(3) The cyclometalation of a variety of aryloxide ligands by low-valent Mo and W systems has been demonstrated; see: (a) Hascall, T.; Murphy, V. J.; Janak, K. E.; Parkin, G, *J. Organomet. Chem.* **2002**, *652*, 37. (b) Hascall, T.; Baik. M. H.; Bridgewater, B. A.; Shin, J. H.; Churchill, D. G.; Friesner, R. A.; Parkin, G. *Chem. Commun.* **2002**, 2644. (c) Rabinovich, D.; Zelman, R.; Parkin, G. *J. Am. Chem. Soc.* **1990**, *112*, 9632. (d) Rabinovich, D.; Zelman, R.; Parkin, G. *J. Am. Chem. Soc.* **1992**, *114*, 4611.

10.1021/om0300934 CCC: $25.00
Publication on Web 10/08/2003

Scheme 1

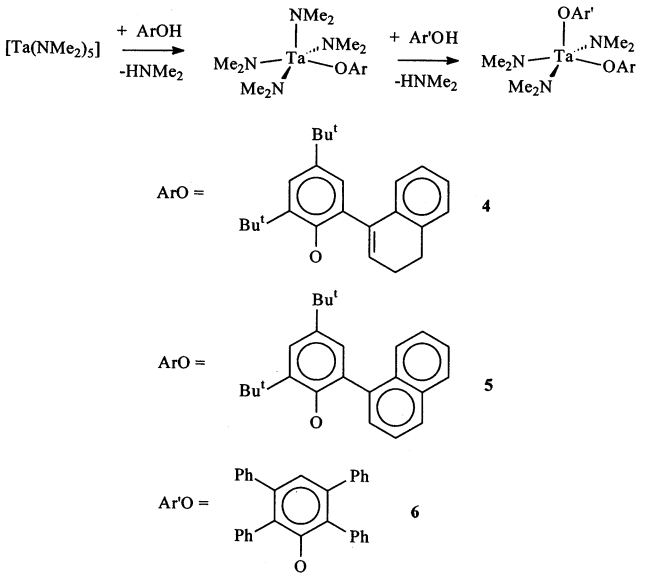

Table 1. Selected Bond Distances (Å) and Angles (deg) for [Ta(OC$_6$H$_2${C$_{10}$H$_8$}-2-Bu$^t_2$-4,6)(NMe$_2$)$_4$] (4)

Ta-O(1)	1.956(3)	Ta−N(4)	1.956(4)
Ta−N(5)	2.013(4)	Ta−N(2)	2.034(4)
Ta−N(3)	2.064(4)		
N(4)−Ta−O(1)	104.0(2)	N(4)−Ta−N(5)	99.2(2)
N(4)−Ta−N(3)	102.8(2)	N(4)−Ta−N(2)	99.7(2)
O(1)−Ta−N(5)	156.8(2)	O(1)−Ta−N(3)	85.8(2)
O(1)−Ta−N(2)	88.7(1)	N(3)−Ta−N(2)	157.5(2)
N(5)−Ta−N(2)	89.5(2)	N(5)−Ta−N(3)	87.1(2)
Ta−O(1)−C(11)	162.4(3)		

Results and Discussion

Synthesis and Characterization of Dimethylamido Compounds. The treatment of hydrocarbon solutions of the compound [Ta(NMe$_2$)$_5$][9] with phenols **1** and **2** leads to the displacement of 1 equiv of dimethylamine and formation of the corresponding mono(aryloxides) **4** and **5** (Scheme 1). Both compounds have been structurally characterized (Tables 1 and 2; Figures 1 and 2). In the solid state they both adopt geometries best described as square pyramidal with an apical dimethylamido ligand and basal aryloxide oxygen. The N(axial)−Ta−N(basal) angles are smaller than the N(axial)−Ta−OAr angle in both **4** and **5**, presumably for steric reasons. It can be seen that the aryloxide wedge is oriented to bring the *o*-aryl ring into the vacant site of the square-based pyramid. The Ta−O−Ar angle is 162° in both compounds. The basal N−Ta−N and O−Ta−N angles are both 157° in **4**. However, in **5** the N−Ta−N angle of 164° is larger than the O−Ta−N angle of 148°. Hence, there is a distinct distortion in **5** toward a trigonal-bipyramidal structure with axial amido groups. The solution ^{1}H NMR spectra of **4** and **5** show a single resonance for the Ta−N*Me*$_2$ protons at

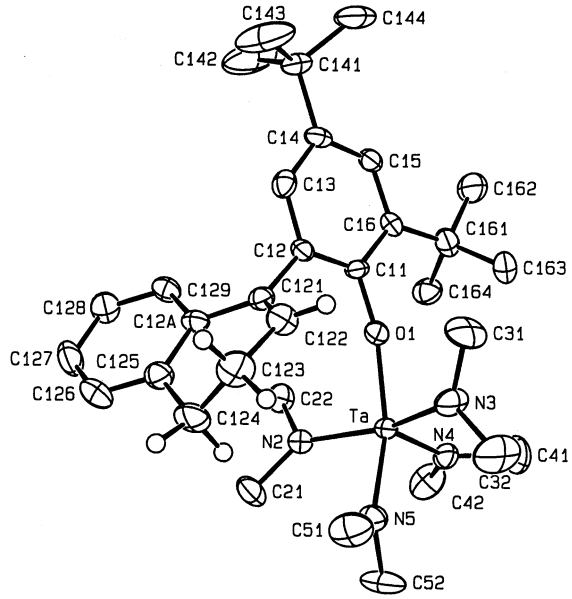

Figure 1. Molecular structure of [Ta(OC$_6$H$_2${C$_{10}$H$_8$}-2-Bu$^t_2$-4,6)(NMe$_2$)$_4$] (**4**).

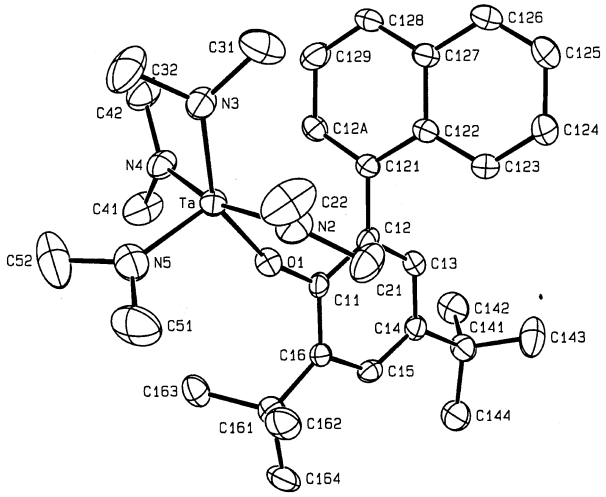

Figure 2. Molecular structure of [Ta(OC$_6$H$_2$Np-2-Bu$^t_2$-4,6)(NMe$_2$)$_4$] (**5**).

Table 2. Selected Bond Distances (Å) and Angles (deg) for [Ta(OC$_6$H$_2$Np-2-Bu$^t_2$-4,6)(NMe$_2$)$_4$] (5)

Ta−O(1)	1.946(4)	Ta−N(4)	2.031(5)
Ta−N(5)	1.939(6)	Ta−N(2)	2.047(6)
Ta−N(3)	1.976(5)		
N(4)−Ta−O(1)	90.0(2)	N(4)−Ta−N(5)	96.8(2)
N(4)−Ta−N(3)	88.1(2)	N(4)−Ta−N(2)	164.2(2)
O(1)−Ta−N(5)	107.3(2)	O(1)−Ta−N(3)	148.0(2)
O(1)−Ta−N(2)	85.6(2)	N(3)−Ta−N(2)	87.6(2)
N(5)−Ta−N(2)	99.0(3)	N(5)−Ta−N(3)	104.7(2)
Ta−O(1)−C(11)	161.8(4)		

(4) Maseras, F.; Lockwood, M. A.; Eisenstein, O.; Rothwell, I. P. *J. Am. Chem. Soc.* **1998**, *120*, 6598.

(5) (a) Lockwood, M. A.; Fanwick, P. E.; Eisenstein, O.; Rothwell, I. P. *J. Am. Chem. Soc.* **1996**, *118*, 2762. (b) Kerschner, J. L.; Rothwell, I. P.; Huffman, J. C.; Streib, W. E. *Organometallics* **1988**, *7*, 1871.

(6) (a) Vilardo, J. S.; Thorn, M. G.; Fanwick, P. E.; Rothwell, I. P. *Chem. Commun.* **1998**, 2425. (b) Thorn, M. G.; Vilardo, J. S.; Fanwick, P. E.; Rothwell, I. P. *Chem. Commun.* **1998**, 2427. (c) Riley, P. N.; Thorn, M. G.; Vilardo, J. S.; Lockwood, M. A.; Fanwick, P. E.; Rothwell, I. P. *Organometallics* **1999**, *18*, 3016. (d) Thorn, M. G.; Vilardo, J. S.; Lee, J.; Hanna, B.; Fanwick, P. E.; Rothwell, I. P. *Organometallics* **2000**, *19*, 5636.

(7) (a) Thorn, M. G.; Fanwick, P. E.; Chesnut, R. W.; Rothwell, I. P. *J. Chem. Soc., Chem. Commun.* **1999**, 2543. (b) Turner, L. E.; Thorn, M. G.; Fanwick, P. E.; Rothwell, I. P. *J. Chem. Soc., Chem. Comm.* **2003**, 1034.

(8) Turner, L. E.; Swartz, R. D.; Thorn, M. G.; Chestnut, R. W.; Fanwick, P. E.; Rothwell, I. P. *J. Chem. Soc., Dalton Trans.*, in press.

(9) Serious safety concerns have been raised dealing with the original procedure: Bradley, D. C.; Thomas, M. *Can. J. Chem.* **1962**, *40*, 1355. For a revised synthesis of [Ta(NMe$_2$)$_5$], see: Vilardo, J. S.; Salberg, M. M.; Parker, J. R.; Fanwick, P. E.; Rothwell, I. P. *Inorg. Chim. Acta* **2000**, *299*, 135. See also: Chesnut, R. W.; Rothwell, I. P.; Banasak Holl, M.; Wolczanski, P. T. *Chem. Eng. News* **1990**, *68*, 2.

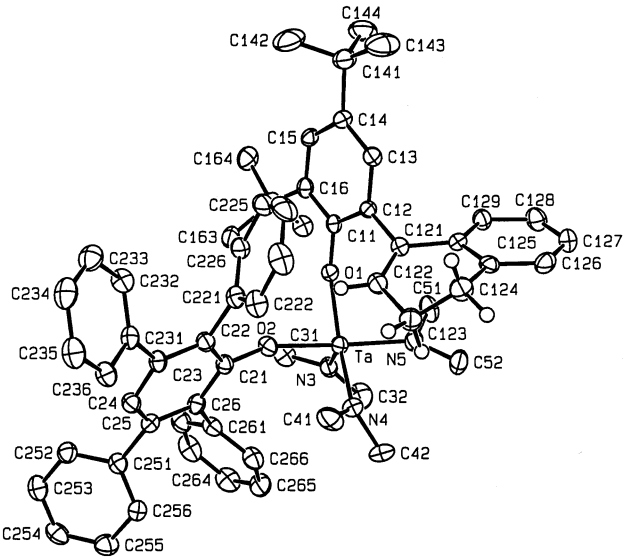

Figure 3. Molecular structure of [Ta(OC_6H_2{$C_{10}H_8$}-2-Bu^t_2-4,6)(OC_6HPh_4-2,3,5,6)($NMe_2)_3$] (**6**).

Table 3. Selected Bond Distances (Å) and Angles (deg) for [Ta(OC_6H_2{$C_{10}H_8$}-2-Bu^t_2-4,6)-(OC_6HPh_4-2,3,5,6)($NMe_2)_3$] (6)

Ta−O(1)	1.948(3)	Ta−O(2)	2.012(3)
Ta−N(3)	1.951(4)	Ta−N(4)	1.995(4)
Ta−N(5)	2.005(3)		
O(1)−Ta−O(2)	85.6(1)	O(1)−Ta−N(3)	102.3(1)
O(1)−Ta−N(4)	148.7(1)	O(1)−Ta−N(5)	93.1(1)
O(2)−Ta−N(4)	85.7(1)	O(2)−Ta−N(3)	101.6(1)
O(2)−Ta−N(5)	167.1(1)	N(3)−Ta−N(4)	108.8(2)
N(3)−Ta−N(5)	91.2(1)	N(4)−Ta−N(5)	88.6(2)
Ta−O(1)−C(11)	154.9(2)	Ta−O(2)−C(21)	159.3(3)

ambient temperatures. Hence, the molecules are highly fluxional in solution, as the solid-state structure would generate nonequivalent dimethylamido ligands. A variable-temperature study of **5** (toluene-d_8) showed that at −80 °C the single resonance split into four equal-intensity singlets at δ 2.38, 2.95, 3.17, and 3.30 ppm. Hence, at low temperature there is not only slow exchange of nonequivalent axial and basal ligands but also restricted rotation about the phenoxy−naphthyl bond. Previous NMR studies of 2,6-bis(1-naphthyl)-phenol have shown the barrier to naphthyl rotation in this molecule can be estimated as 18.0(5) kcal mol^{-1} at 67 °C. The barrier increases significantly in metal derivatives of *o*-naphthylphenoxides.

Addition of 2,3,5,6-tetraphenylphenol to a solution of **4** leads to a further displacement of 1 equiv of dimethylamine and formation of the bis(aryloxide) **6** (Scheme 1). The solid-state structure of **6** (Table 3, Figure 3) displays a metal coordination geometry very similar to that of **5**, except that there are now two, mutually cis basal aryloxide ligands. The O−Ta−O angle is very small at 86°. The basal position of the distorted square pyramid, trans O−Ta−N angles of 149 and 167°, is occupied by the 3,4-dihydronaphthyl substituent (Figure 3). Bis(aryloxide) tris(amides) of niobium or tantalum that have been structurally characterized are [Nb(OC_6H_2Ph-2-Bu^t_2-4,6)$_2$($NMe_2)_3$][10] and the 2,2′-methylenebis(4-methyl-6-*tert*-butylphenoxide) [Ta{(OC_6H_2Me-4-Bu^t-6)$_2CH_2$}($NMe_2)_3$].[11] Surprisingly, compound **6** is structurally very similar to the chelated tantalum compound and significantly different from the niobium example. In the niobium compound the two aryloxides are mutually trans with an O−Nb−O angle of 145°, whereas in the chelated compound this angle is 85°, almost identical with that found in **6**. These compounds highlight the fact that there is a great deal of variety in the solid-state structures that can be adopted by these mixed aryloxy amides, with geometries being very close in energy.

The substrate [Ta($NMe_2)_5$] reacts with inden-3-ylphenol **3** to initially form the tetrakis(dimethylamido) compound **7** (Scheme 2). The spectroscopic properties of **7** indicate that the indenyl ring remains protonated, and presumably a structure is formed very similar to that observed for **4** and **5**. However, when compound **7** was heated to 100 °C under vacuum, displacement of a second 1 equiv of dimethylamine occurred with formation of the tris(amide) **8** (Scheme 2). In the solid state **8** (Table 4, Figure 4) can be seen to contain a five-coordinate tantalum atom with a new chelate ring. The coordination geometry about tantalum is best described as trigonal bipyramidal with an oxygen and amido group in the axial positions: O−Ta−N = 170°. The equatorial ligands are two amido nitrogens and a carbon atom on the aryloxide chelate. This carbon atom, C(121), is the indenyl carbon bound directly to the phenoxide nucleus, leading to a five-membered metallacycle. The structural parameters for the tantalum-bound indenyl ring show that there is a localized double bond between C(122) and C(123) (Figure 4). Hence, both deprotonation (CH bond activation) and tautomerization of the original inden-3-yl ring has occurred. The Ta−C(121) distance of 2.285(9) Å is consistent with a Ta−C(sp^3) σ bond. The distance is almost identical with the value of 2.216(3) Å reported for the Ta−C bond in [Ta($OC_6H_3Pr^i$-CMe_2)($OC_6H_3Pr^i_2$-2,6)$_3$], containing a cyclometalated 2,6-diisopropylphenoxide ligand.[12] The Ta−O−C angles are 122° in this compound and 123° in **8**. Hence, all of the structural data are consistent with an η^1-indenyl ring being present in **8**. Previous examples of transition-metal η^1-indenyl compounds involved diruthenium compounds.[13] More recently examples of η^1-indenyl rings bound to titanium[14] and rhenium[15] have been reported.

In the ^{1}H NMR spectrum of **8** at ambient temperatures, the N*Me*$_2$ protons appear as a single broad resonance, indicating that the molecule is fluxional on the NMR time scale. As the temperature is lowered, the signal broadens and splits at −55 °C into four singlets of intensity ratio 2:2:1:1 (Figure 5). We interpret this observation as a freezing out of the trigonal-bipyramidal structure on the NMR time scale, with the methyl groups of the axial NMe_2 group being nonequivalent due to restricted rotation (Scheme 2, Figure 5).

Reactivity of the Dimethylamido Compounds. The fact that the indenyl ring in **8** adopts an η^1 bonding

(10) Visciglio, V. M.; Fanwick, P. E.; Rothwell, I. P. *Inorg. Chim. Acta* **1993**, *211*, 203.

(11) Chisholm, M. H.; Huang, J.-H.; Huffman, J. C.; Streib, W. E.; Tiedtke, D. *Polyhedron* **1997,** *16*, 2941.

(12) Yu, J. S.; Felter, L.; Potyen, M. C.; Clark, J. R.; Visciglio, V. M.; Fanwick, P. E.; Rothwell, I. P. *Organometallics* **1996**, *15*, 4443.

(13) Blenkiron, P.; Enright, G. D.; Taylor, N. J.; Carty, A. J. *Organometallics* **1996,** *15*, 2855.

(14) Guerin, F.; Beddie, C. L.; Stephan, D. W.; Spence, R. E. v. H.; Wurz, R. *Organometallics* **2001,** *20*, 3466.

(15) Deck, P. A.; Fronczek, F. R. *Organometallics* **2000,** *19*, 327.

Scheme 2

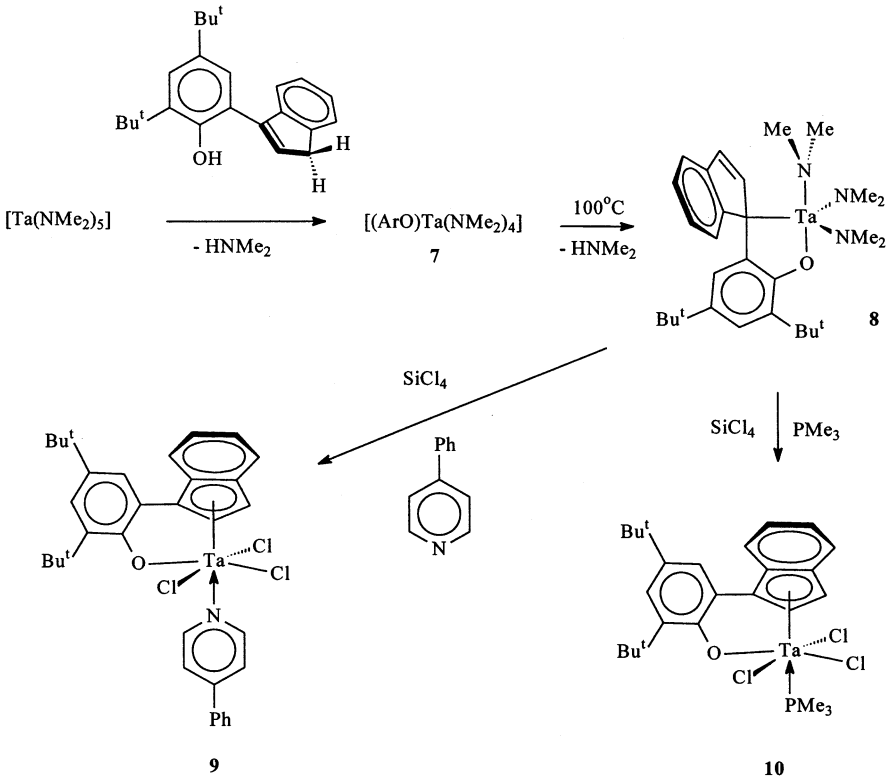

Table 4. Selected Bond Distances (Å) and Angles (deg) for [Ta(OC$_6$H$_2${η^1-C$_9$H$_6$}-2-Bu$^t_2$-4,6)(NMe$_2$)$_3$] (8)

Ta−O(1)	2.025(7)	C(16)−C(121)	1.51(1)
Ta−N(2)	1.95(1)	C(121)−C(122)	1.49(1)
Ta−N(3)	1.95(1)	C(122)−C(123)	1.33(2)
Ta−N(4)	2.005(8)	C(123)−C(124)	1.47(2)
Ta−C(121)	2.285(9)	C(124)−C(129)	1.42(1)
O(1)−C(11)	1.36(1)	C(129)−C(121)	1.49(1)
C(11)−C(16)	1.39(1)		
Ta−O(1)−C(11)	122.7(6)	N(2)−Ta−N(4)	92.8(4)
O(1)−Ta−N(2)	90.8(3)	N(2)−Ta−C(121)	123.6(4)
O(1)−Ta−N(3)	93.8(4)	N(3)−Ta−N(4)	92.9(4)
O(1)−Ta−N(4)	169.9(3)	N(3)−Ta−C(121)	117.7(4)
O(1)−Ta−C(121)	75.4(3)	N(4)−Ta−C(121)	94.7(3)
N(2)−Ta−N(3)	117.6(5)		

mode can be ascribed to the presence of the dimethylamido ligands. These groups form very stable bonds to early d-block metals in high oxidation states due to the presence of nitrogen p to metal d π-bonding.[16] This bonding requires empty d orbitals of the correct symmetery into which the electron density on the nitrogen atom can be donated. The formation of an η^3-indenyl or η^5-indenyl group would presumably reduce and weaken these interactions.

Replacement of the three dimethylamido ligands in **8** by chloride groups was achieved by reaction with $SiCl_4$ (Scheme 2). Spectroscopically it was not possible to determine the hapticity of the indenyl ring in the trichloride product (Figure 6). To isolate and characterize the resulting trichloride, it was found necessary to add the donor ligands 4-phenylpyridine (forming **9**) and PMe_3 (**10**). The solid-state structure of **9** was determined to fully characterize the bonding of the indenyl ring (Figure 7, Table 5). The molecular structure is best

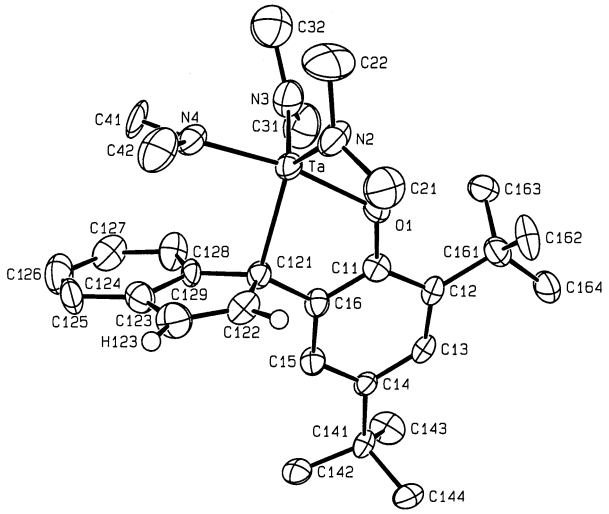

Figure 4. Molecular structure of [Ta(OC$_6$H$_2${η^1-Ind}-2-Bu^t-4,6)(NMe$_2$)$_3$] (**8**).

described as distorted octahedral, with the indenyl ring occupying an axial site trans to the pyridine nitrogen. The three chlorides and aryloxide oxygen are bent toward the pyridine nitrogen with angles close to only 80°. Related structures have been found for the previously reported adducts [CpNbCl$_4$(PMePh$_2$)][17] and [(MeCp)TaCl$_4$(H$_2$PC$_6$H$_2$Pr$^i_3$-2,4,6)],[18] which both have P−M−Cl angles slightly less than 80°. Previously in our group we have isolated and structurally characterized the mono(aryloxides) [CpNbCl$_3$(OC$_6$HPh$_2$-2,6-Bu$^t_2$-3,5)] and [Cp*TaCl$_3$(OC$_6$HPh$_2$-2,6-Bu$^t_2$-3,5)]. The Ta−O distance of 1.968(3) Å in **9** is slightly shorter than the

(16) Riley, P. N.; Fanwick, P. E.; Rothwell, I. P. *J. Chem. Soc., Dalton Trans.* **2001**, 181.

(17) Fettinger, J. C.; Keogh, D. W.; Poli, R. *Inorg. Chem.* **1995,** *34*, 2343.

(18) Hadi, G. A. A.; Fromm, K.; Blaurock, S.; Jelonek, S.; Hey-Hawkins, E. *Polyhedron* **1997,** *16*, 721.

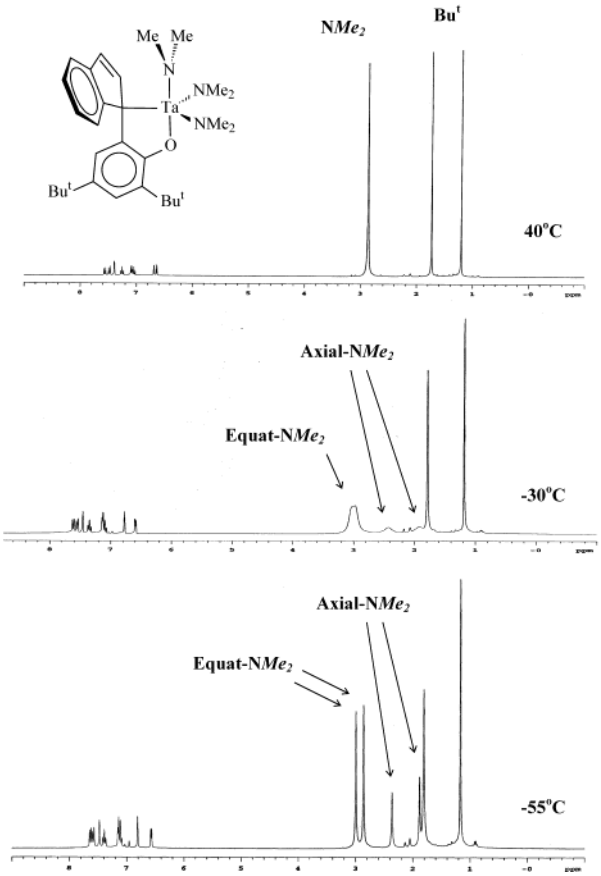

Figure 5. ^{1}H NMR (toluene-d_8) spectrum of [Ta(OC$_6$H$_2$-{η^1-Ind}-2-Bu^t-4,6)(NMe$_2$)$_3$] (**8**) at 40, −30, and −55 °C.

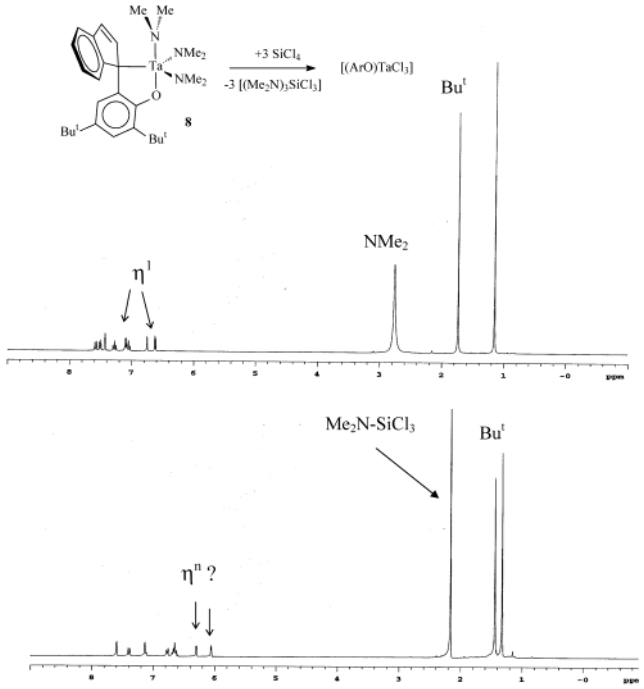

Figure 6. ^{1}H NMR (C_6D_6) spectrum of the reaction mixture of [Ta(OC$_6$H$_2${η^1-Ind}-2-Bu^t-4,6)(NMe$_2$)$_3$] (**8**) with SiCl$_4$.

2.025(7) Å distance found in **8**, consistent with an increase in electron deficiency of the metal. There is also a corresponding increase in interaction with the indenyl ring upon replacing the dimethylamido groups by chloride ligands. The details of this interaction can be

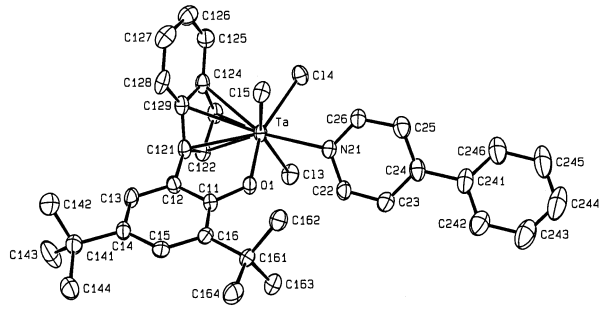

Figure 7. Molecular structure of [Ta(OC$_6$H$_2${η^5-Ind}-2-Bu^t-4,6)(NC$_6$H$_4$Ph-4)Cl$_3$] (**9**).

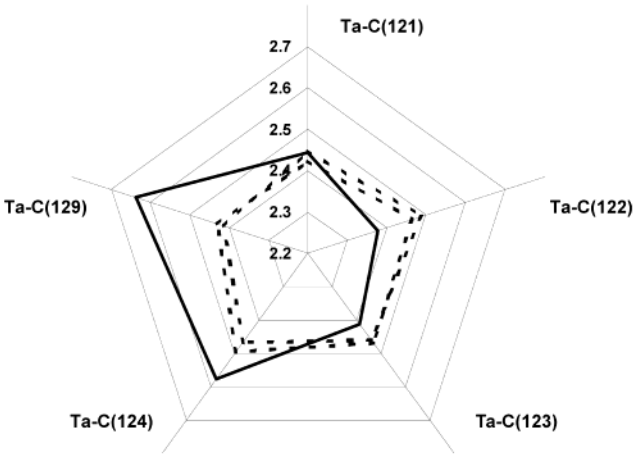

Figure 8. "Radar" plot of the Ta−C(indenyl) (solid line) and Ta−Cp (dashed line) distances in compound **9**, [CpNbCl$_4$(PMePh$_2$)], and [(MeCp)TaCl$_4$(H$_2$PC$_6$H$_2$Pr$^i_3$-2,4,6)]. The coordination is exaggerated by using a plot scale of 2.2−2.7 Å from the metal center.

Table 5. Selected Bond Distances (Å) and Angles (deg) for [Ta(OC$_6$H$_2${η^5-C$_9$H$_6$}-2-Bu^t-4,6)-(NC$_5$H$_4$Ph-4)Cl$_3$] (9)

Ta−O(1)	1.968(3)	Ta−C(124)	2.578(5)
Ta−N(21)	2.326(4)	Ta−C(129)	2.636(4)
Ta−Cl(3)	2.436(1)	C(121)−C(122)	1.415(6)
Ta−Cl(4)	2.449(1)	C(122)−C(123)	1.406(7)
Ta−Cl(5)	2.386(1)	C(123)−C(124)	1.420(7)
Ta−C(121)	2.443(4)	C(124)−C(129)	1.422(6)
Ta−C(122)	2.378(4)	C(129)−C(121)	1.426(7)
Ta−C(123)	2.412(4)		
Ta−O(1)−C(11)	129.0(3)	Cl(4)−Ta−Cl(5)	85.80(4)
O(1)−Ta−Cl(3)	90.75(9)	Cl(4)−Ta−N(21)	80.34(9)
O(1)−Ta−Cl(4)	157.37(9)	Cl(5)−Ta−N(21)	78.51(9)
O(1)−Ta−Cl(5)	87.24(9)	N(21)−Ta−C(121)	148.3(1)
O(1)−Ta−N(21)	77.2(1)	N(21)−Ta−C(122)	148.9(2)
Cl(3)−Ta−Cl(4)	86.52(4)	N(21)−Ta−C(123)	151.7(2)
Cl(3)−Ta−Cl(5)	154.85(4)	N(21)−Ta−C(124)	154.1(1)
Cl(3)−Ta−N(21)	76.6(1)	N(21)−Ta−C(129)	152.5(1)

clarified by inspection of the "Radar" plot shown in Figure 8. It can be seen that there is a distinct distortion toward η^3 bonding for the indenyl ring in **9** with none of the contacts as short as the 2.285(9) Å distance observed in **8**. The Ta−C(indenyl) distances can be compared to those reported for [CpNbCl$_4$(PMePh$_2$)] and [(MeCp)TaCl$_4$(H$_2$PC$_6$H$_2$Pr$^i_3$-2,4,6)] mentioned previously, where the M−C(cyclopentadienyl) distances are all similar (Figure 8). As expected, the slippage of the indenyl ring involves a distinct elongation of the Ta−C distances to the two aromatic carbon atoms. The "slip value" has been defined as $\Delta = d\{\text{M−C(3a,7a)}\}_{av} - d\{\text{M−C(1,3)}\}_{av}$.[19] This corresponds to $\Delta = d\{$M−C(124,-

Table 6. Crystal Data and Data Collection Parameters

	4	5	6	8	9
formula	$C_{32}H_{53}N_4OTa$	$C_{60}H_{68}N_3O_2Ta$	$C_{32}H_{51}N_4OTa$	$C_{29}H_{44}N_3OTa$	$C_{34}H_{35}Cl_3NOTa$
formula wt	690.75	1044.18	688.74	631.64	760.97
space group	$P2_1/n$ (No. 14)	$P2_1/n$ (No. 14)	$P\bar{1}$ (No. 2)	$P\bar{1}$ (No. 2)	$P2_1/n$ (No. 14)
a, Å	12.2706(2)	15.7906(3)	10.4794(9)	9.6679(5)	13.5784(3)
b, Å	20.4323(5)	14.8876(3)	11.6107(6)	12.1261(6)	14.7969(3)
c, Å	13.3871(3)	23.0163(6)	14.392(1)	13.9575(4)	16.9241(4)
α, deg	90	90	105.499(5)	86.118(3)	90
β, deg	101.257(1)	107.864(1)	104.203(4)	72.704(3)	111.549(1)
γ, deg	90	90	96.141(5)	67.257(2)	90
V, Å^3	3291.8(2)	5149.9(4)	1438.8(2)	1438.8(2)	3162.7(2)
Z	4	4	2	2	4
ρ_{calcd}, g cm^{-3}	1.458	1.347	1.423	1.458	1.598
temp, K	193.	193.	193.	203.	193
radiation (wavelength)			Mo Kα (0.710 73 Å)		
R	0.033	0.043	0.042	0.061	0.038
R_w	0.091	0.093	0.101	0.153	0.095

129)}$_{av}$ − *d*{M−C(121,123)}$_{av}$ in the labeling used here. For compound **8** Δ = 0.179 Å. For a "true η^5-indenyl" this value would be close to 0 Å, whereas values of ∼0.75 Å are calculated for "true η^3-indenyl" compounds.[19] Hence, although definitely slipped toward η^3-indenyl, compound **8** is not as "slipped" as possible. As the database of structurally characterized group 5 metal indenyl compounds increases, there will undoubtedly be a spectrum of interactions in response to the electronic and steric demands of the metal center.

Experimental Section

General Remarks. All manipulations were carried out using standard syringe, Schlenk line, and glovebox techniques.[20] Benzene, toluene, ether, THF, and *n*-hexane were dried over sodium benzophenone ketyl and were freshly distilled before use. Pentane was dried over sodium ribbon. The substrate [Ta(NMe$_2$)$_5$] was obtained by literature procedures. *Caution!* Explosions have been associated with the synthesis of [Ta(NMe$_2$)$_5$].[9] *o*-Dihydronaphthyl-, 1-naphthyl-, and inden-3-ylphenols [HOC$_6$H$_2$Ar-2-Bu$^t_2$-4,6] (Ar = C$_{10}$H$_9$ (**1**), C$_{10}$H$_7$ (Np; **2**), C$_9$H$_7$ (**3**)) were prepared according to literature procedures.[6,8] ^{1}H NMR spectra were recorded on a Varian INOVA-300 NMR spectrometer or a Bruker DRX-500 NMR spectrometer and were referenced to residual protio impurities in the NMR solvent. ^{13}C NMR spectra were recorded on a Bruker DRX-500 NMR spectrometer at 125.7 MHz and were internally referenced to the solvent signal.

Synthesis of [Ta(OC$_6$H$_2${C$_{10}$H$_8$}-2-Bu$^t_2$-4,6)(NMe$_2$)$_4$] (4). To a solution of [Ta(NMe$_2$)$_5$] (0.50 g, 1.25 mmol) in benzene (8.0 mL) was slowly added 2-(3,4-dihydro-1-naphthyl)-4,6-di-*tert*-butylphenol (0.416 g, 1.25 mmol). The mixture was stirred for 6 h, and the solvent was removed under vacuum, resulting in an "off white" powder. Pentane (2.0 mL) was added to the powder, and cooling to −15 °C resulted in the precipitation of **4** as an off-white solid. Crystals suitable for X-ray diffraction were obtained from benzene/pentane solutions. Yield: 0.20 g (23%). Anal. Calcd for $C_{32}H_{53}N_4OTa$: C, 55.64; H, 7.73; N, 8.11. Found: C, 55.44; H, 7.42; N, 8.00. ^{1}H NMR (C$_6$D$_6$, 30 °C): *δ* 6.9−7.6 (aromatics); 3.48 (br, C*H*$_2$); 3.13 (s, N*Me*$_2$); 2.75 (m), 2.90 (m, C*H*$_2$C*H*$_2$); 1.64 (s), 1.29 (s, C*Me*$_3$). Selected ^{13}C NMR (C$_6$D$_6$, 30 °C): *δ* 157.5 (Ta−O−*C*); 47.3 (N*Me*$_2$); 39.1 (C*H*$_2$); 35.8, 34.4 (*C*Me$_3$); 31.9, 30.5 (C*Me*$_3$); 28.5, 24.2 (*C*H$_2$CH$_2$).

Synthesis of [Ta(OC$_6$H$_2$Np-2-Bu$^t_2$-4,6)(NMe$_2$)$_4$] (5). To a solution of [Ta(NMe$_2$)$_5$] (0.50 g, 1.25 mmol) in benzene (8.0 mL) was slowly added 2-(1-naphthyl)-4,6-di-*tert*-butylphenol (0.410 g, 1.24 mmol). The mixture was stirred for 6 h, and the solvent was removed under vacuum, resulting in an "off white" powder. Pentane (2.0 mL) was added to the powder, and cooling to −15 °C resulted in the precipitation of **6** as an off-white solid. Crystals suitable for X-ray diffraction were obtained from benzene/pentane solutions. Yield: 0.19 g (22%). Anal. Calcd for $C_{32}H_{51}N_4OTa$: C, 55.21; H, 7.46; N, 8.13. Found: C, 55.26; H, 6.75; N, 8.46. ^{1}H NMR (C$_6$D$_6$, 30 °C): *δ* 7.80−7.10 (m, 19H, aromatic region); 3.00 (s, 24H, N*Me*$_2$); 1.32 (s, 18H, C(CH$_3$)$_3$).

Synthesis of [Ta(OC$_6$H$_2${C$_9$H$_7$}-2-Bu$^t_2$-4,6)(NMe$_2$)$_4$] (7). A sample of [Ta(NMe$_2$)$_5$] (500 mg, 1.25 mmol) was dissolved in benzene. This mixture was stirred as 2-(inden-3-yl)-4,6-di-*tert*-butylphenol (400 mg, 1.25 mmol) dissolved in benzene was slowly added. The mixture was stirred for 1 h and then evacuated to dryness, affording a yellow glassy solid. Addition of a minimal amount of pentane resulted in the formation of white crystals (190 mg, 22%). Anal. Calcd for $C_{31}H_{51}N_4OTa$: C, 55.02; H, 7.60; N, 8.28. Found: C, 54.76; H, 7.64; N, 7.83. ^{1}H NMR (C$_6$D$_6$, 30 °C): *δ* 7.17−7.73 (aromatics); 6.60 (t, C*H*); 3.48 (br, C*H*$_2$); 3.15 (s, N*Me*$_2$); 1.70 (s), 1.37 (s, C*Me*$_3$). Selected ^{13}C NMR (C$_6$D$_6$, 30 °C): *δ* 157.2 (Ta−O−*C*); 47.1 (N*Me*$_2$); 39.1 (C*H*$_2$); 35.8, 34.5 (*C*Me$_3$); 31.8, 30.3 (C*Me*$_3$).

Synthesis of [Ta(OC$_6$H$_2${η^1-Ind}-2-Bu^t-4,6)(NMe$_2$)$_3$] (8). A sample of [Ta(NMe$_2$)$_5$] (1.0 g, 2.49 mmol) was dissolved in benzene. This mixture was stirred as 2-(3-dihydroindenyl)-4,6-di-*tert*-butylphenol (800 mg, 2.5 mmol) dissolved in benzene was slowly added. The mixture was stirred for 1 h at room temperature and then heated at 100 °C for 45 min and finally evacuated to dryness, affording a yellow glassy solid. Recrystallization from benzene/pentane afforded yellow crystals (350 mg, 23%). Anal. Calcd for $C_{29}H_{44}N_3OTa$: C, 55.15; H, 7.02; N, 6.65. Found: C, 54.93; H, 6.91; N, 6.36. ^{1}H NMR (C$_6$D$_6$, 30 °C): *δ* 7.58 (d), 7.51 (d), 7.28 (t), 7.05 (t, C$_6$*H*$_4$); 7.43 (d), 6.76 (d, *m*-*H*); 7.10 (d), 6.62 (d, C$_5$*H*$_2$); 2.76 (br, N*Me*$_2$); 1.74 (s), 1.15 (s, C*Me*$_3$). ^{1}H NMR (C$_7$D$_8$, 40 °C): *δ* 7.56 (d), 7.49 (d), 7.25 (t), 7.05 (t, C$_6$*H*$_4$); 7.39 (d), 6.69 (d, $^4J(^1H-^1H)$ = 1.7 Hz, *m*-*H*); 7.09 (d), 6.64 (d, C$_5$*H*$_2$); 2.87 (s, N*Me*$_2$); 1.73 (s), 1.21 (s, C*Me*$_3$). ^{1}H NMR (C$_7$D$_8$, −30 °C): *δ* 6.59−7.63 (aromatics); 2.98 (br), 2.43 (br), 1.92 (br, N*Me*$_2$); 1.79 (s), 1.18 (s, C*Me*$_3$). ^{1}H NMR (C$_7$D$_8$, −55 °C): *δ* 6.57−7.64 (aromatics); 3.00 (s, 6H), 2.86 (s, 6H), 2.36 (s, 3H), 1.88(s, 3H, N*Me*$_2$); 1.81 (s), 1.17 (s, C*Me*$_3$). Selected ^{13}C NMR (C$_6$D$_6$, 30 °C): *δ* 163.0 (Ta−O−*C*); 103.4 (Ta−*C*); 44.5 (N*Me*$_2$); 35.1, 34.5 (*C*Me$_3$); 32.0, 30.4 (C*Me*$_3$).

Synthesis of [Ta(OC$_6$H$_2${η^3-Ind}-2-Bu^t-4,6)(NC$_5$H$_4$Ph-4)-Cl$_3$] (9). A solvent-sealed NMR tube was charged with [Ta(OC$_6$H$_2${η^1-Ind}-2-Bu^t-4,6)(NMe$_2$)$_3$] (**8**) and d_6-benzene, affording a yellow solution to which was added several drops of SiCl$_4$. The solution immediately became red. Adding a few crystals of 4-phenylpyridine and layering with pentane gave X-ray-quality red crystals. Anal. Calcd for $C_{34}H_{35}Cl_3NOTa$: C, 53.67; H, 4.64; N, 1.84. Found: C, 53.01; H, 4.71; N, 1.78. ^{1}H NMR (C$_6$D$_6$, 30 °C): *δ* 10.0 (d, *o*-NC$_6$*H*$_4$Ph-4); 6.81−7.76 (aromatics); 7.19 (d), 6.45 (d, $^3J(^1H-^1H)$ = 3.2 Hz, η^5-C*H*); 1.36 (s), 1.30 (s,

(19) Westcott, S. A.; Kakkar, A. K.; Stringer, G.; Taylor, N. J.; Marder, T. B. *J. Organomet. Chem.* **1990,** *394*, 777.

(20) Shriver, D. F.; Drezdzon, M. A. *The Manipulation of Air-Sensitive Compounds*, 2nd ed.; Wiley: New York, 1986.

C*Me*$_3$). Selected ^{13}C NMR (C_6D_6, 30 °C): δ 172.1 (Ta−O−*C*); 104.9 (Ta−*C*); 35.4, 34.9 (*C*Me$_3$); 31.9, 30.4 (C*Me*$_3$).

Synthesis of [Ta(OC$_6$H$_2${η^n-Ind}-2-Bu^t-4,6)(PMe$_3$)Cl$_3$] (10). A solvent-sealed NMR tube was charged with [Ta(OC$_6$H$_2$-{η^1-Ind}-2-Bu^t-4,6)(NMe$_2$)$_3$] (**8**) and d_6-benzene, affording a yellow solution to which was added several drops of $SiCl_4$. The solution immediately became red. Adding 1 drop of trimethylphosphine and layering with pentane gave orange crystals. Anal. Calcd for $C_{26}H_{35}Cl_3POTa$: C, 45.80; H, 5.17. Found: C, 45.51; H, 5.09. ^{1}H NMR (C_6D_6, 30 °C): δ 6.74−7.63 (aromatics); 6.99 (d), 6.24 (d, $^3J(^1H-^1H) = 3.2$ Hz, η^5-C*H*); 1.48 (d, $^2J(^1H-^{31}P) = 10.5$ Hz, P*Me*$_3$); 1.40 (s), 1.34 (s, C*Me*$_3$). ^{31}P NMR (C_6D_6, 30 °C): δ 8.74 (s, *P*Me$_3$).

X-ray Data Collection and Reduction. Crystal data and data collection parameters are contained in Table 6. A suitable crystal was mounted on a glass fiber in a random orientation under a cold stream of dry nitrogen. Preliminary examination and final data collection were performed with Mo Kα radiation ($\lambda = 0.710\ 73$ Å) on a Nonius Kappa CCD instrument. Lorentz and polarization corrections were applied to the data.[21] An empirical absorption correction using SCALEPACK was applied.[22] Intensities of equivalent reflections were averaged. The structure was solved using the structure solution program PATTY in DIRDIF92.[23] The remaining atoms were located in succeeding difference Fourier syntheses. Hydrogen atoms were included in the refinement but restrained to ride on the atom to which they are bonded. The structure was refined in full-matrix least squares, where the function minimized was $\sum w(|F_o|^2 - |F_c|^2)^2$ and the weight w is defined as $w = 1/[\sigma^2(F_o^2) + (0.0585P)^2 + 1.4064P]$ ($P = (F_o^2 + 2F_c^2)/3$). Scattering factors were taken from ref 24. Refinement was performed on a AlphaServer 2100 using SHELX-97.[25] Crystallographic drawings were done using ORTEP programs.[26]

Acknowledgment. We thank the National Science Foundation (Grant No. CHE-0078405) for financial support of this research.

Supporting Information Available: Tables of crystallographic data for **4**−**6**, **8**, and **9**. This material is available free of charge via the Internet at http://pubs.acs.org.

OM0300934

(21) McArdle, P. C. *J. Appl. Crystallogr.* **1996**, *239*, 306.
(22) Otwinowski, Z.; Minor, W. *Methods Enzymol.* **1996**, 276.
(23) Beurskens, P. T.; Admirall, G.; Beurskens, G.; Bosman, W. P.; Garcia-Granda, R S.; Gould, O.; Smits, J. M. M.; Smykalla, C. The DIRDIF92 Program System; Technical Report; Crystallography Laboratory, University of Nijmegen, Nijmegen, The Netherlands, 1992.
(24) *International Tables for Crystallography*; Kluwer Academic: Dordrecht, The Netherlands, 1992; Vol. C, Tables 4.2.6.8 and 6.1.1.4.
(25) Sheldrick, G. M. SHELXS97. A Program for Crystal Structure Refinement; University of Gottingen, Gottingen, Germany, 1997.
(26) Johnson, C. K. ORTEPII; Report ORNL-5138; Oak Ridge National Laboratory, Oak Ridge, TN, 1976.